Lithofacies Discrimination based on Elastic Attribute Analysis and Geological Properties of Maastrichtian Reservoir of High Block from Roncador Field – Campos Basin

Mario Florêncio Barreto Paiva[1], Wagner Moreira Lupinacci[1]

[1]Exploratory Interpretation and Reservoir Characterization Group (GIECAR), Department of Geology and Geophysics, Universidade Federal Fluminense, Niterói, RJ,Brazil

This paper was prepared for presentation during the 17th International Congress of the Brazilian Geophysical Society held in Rio de Janeiro, Brazil,16-19August 2021.

Abstract

The use of elastic attributes derived from seismic impedances is a powerful methodology to extract physical and geological information. However, impedance calculation often lacks geological information and becomes a purely mathematical process. Therefore, it is up to the interpreter to associate the physical-mathematical processes with the geological effects, which can lead to ambiguous or even erroneous interpretations, due to the nature of the process. Thus, we propose a study of the elastic responses based on the geological properties of the rocks through an analysis of the elastic attributes, which proved to be capable of capturing such effects accurately and easy implementation. The methodology is based on the analysis of depth trends, which in this case, revealed the dependence of elastic properties on the effects of geology. We investigated the impact on seismic amplitudes and elastic impedances. From elastic impedance contrasts, we found out that the AVO impedance technique (AVOI) proved to be adequate. From this finding, an attribute from the projection of elastic impedances AI *versus* EI2 was generated, which was successful in characterizing and separating the lithofacies of the Roncador Field, Campos Basin.

Introduction

The use of elastic attributes is common in the oil industry and its beginning dates from the 1980s with the work of Aki & Richard (1980). Over the years, methodologies were developed improving this process and the seismic inversion techniques were adopted as essential part in reservoir characterization workflows. However, it is necessary for the interpreter to insert relevant information to add a geological meaning to the impedance volumes.

The level of geological details inserted depends on the methodology used. In this sense, the maximum amount of geological and physical information must be considered to optimize the cost versus benefit ratio of the seismic inversion process. Some methodologies, such as geostatistical inversions can generate impedance volumes highly detailed (Avseth et al., 2005). Though, the time required to prepare the data and the computational cost can be prohibitive.

This work presents a methodology capable of capturing geological and physical properties of rocks from lithofacies classification. Our analysis resulted in an elastic attribute derived on the combination of elastic impedances for lithofacies characterization and the geological effects with this modeling. We applied this methodology in five wells located in the High Block of the Roncador Field - Campos Basin.

Roncador Field is located at the northern portion of the Campos Basin, approximately 125km of the coast of the state of Rio de Janeiro, with water column varying from 1500 to 1900m (Pádua *et al*., 1998). According ANP (2021), Roncador Field is responsible for the fifth major oil production daily in Brazil, being the biggest siliciclastic productor in activity currently.

The target of this study is the turbiditic reservoir RO 330. It is composed of trough confined gravel/sand-rich lobes of Maastrichtian age, being the main productor system in this field (Bruhn *et al*., 2003). These turbidites sandstones are located at Carapebus Formation, Tamoios Member, having an average porosity and oil saturation up to 29% and 82% respectively. The oil gravity shows API between 17º and 31º units (Rangel *et a*l., 1998).

Methodology

The analysis of the depth trends (TVDml) for the P wave velocity (Vp) allowed to verify the existence of two main trends for reservoir and non-reservoir rocks, evidencing geological effects, where such effects are related to diagenesis. Mechanical compaction, cementation and sort are the main mechanism responsible for the variation in porosity and mineralogy (Paiva, 2021), impacting the elastic properties of rocks (Figure 1).

The lithofacies were classified considering the effects of diagenesis on the porosity and their relationship with the P wave velocity, to capture the geological effects on the elastic response as shown in Figure 2.

When applying cementation rock physics models[1] (Avseth et al., 2005) on the reservoir facies, Paiva (2021) showed that the difference in velocity for Sand C and Sand B is due to the cementation amount, where Sand C is more cemented than Sand B, with 1% and 0.5% cement, respectively.

---

[1] Constant – Cement Model
Contact - Cement Model

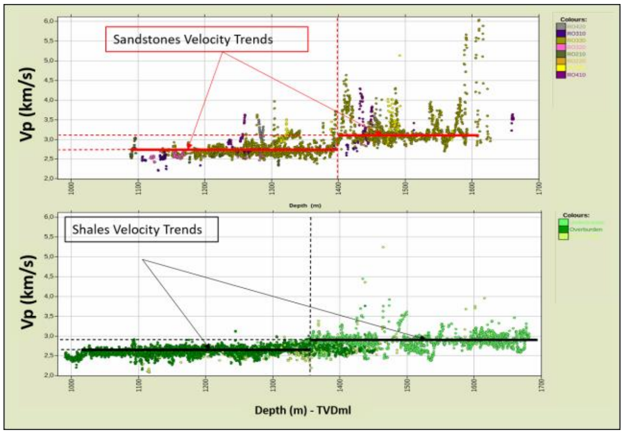

Figure 1 – Velocity trends for reservoir and non-reservoir rocks.

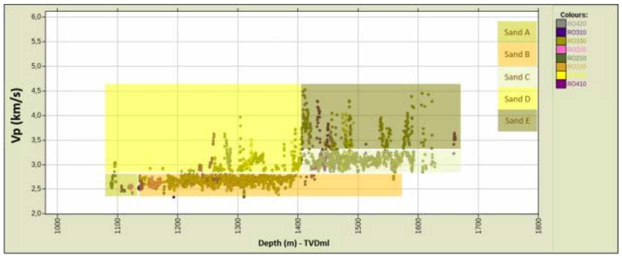

Figure 2 - Lithofacies classification for reservoir rocks based on P wave velocity response.

Sand D and Sand E have the same cementation degree of Sand C. In this way, cementation does not play a major role. The increase in velocity for the Sand D and Sand E can be explained by the sorting, in which the smaller grains fill the porous space among the larger grains, consequently decreasing the porosity.

We performed the lithofacies classification for non-reservoir rocks with the aid of the lithology logs generated from the well documentation and the petrophysical curves of clay volume (Vclay) and porosity (PHIT). We defined non-reservoir facies as Overburden, Underburden and intra-reservoir. Overburden interval are the shales above the reservoir RO 330. The Underburden interval are the shales below reservoir RO300 and the intra-reservoir facies are the shales laminations identified inside the RO 330.

With the lithofacies defined, the next step was to verify the effects of geological and physical properties on the seismic amplitudes. This process involved the calculation of reflection coefficients for the insitu and 100% water saturated cases, comparing with the real and synthetic amplitudes along the selected interfaces. These interfaces were chosen including the Top and Base of RO330 and a secondary interface that split the reservoir in RO330A and RO330B, where they are indicated for well 9 RO 31A RJS according to Figure 3.

We used a deterministic wavelet extracted from seismic data through the methodology described by White & Simm (2003). The wavelet presented a phase rotation of 40 ° and a time delay of -4ms. The synthetic amplitudes calculated based on modeled reflection coefficients followed the expected behavior regarding AVO plot, in which showed an excellent correlation with real data (Figure 4) for interfaces 1 and 2.

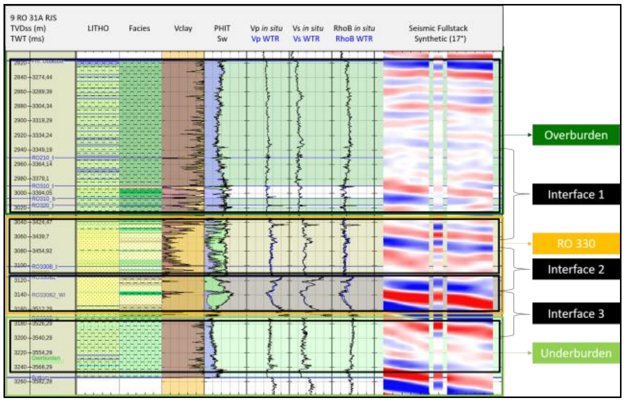

Figure 3 – Interest zones and interfaces defined to Well 9 RO 31A RJS.

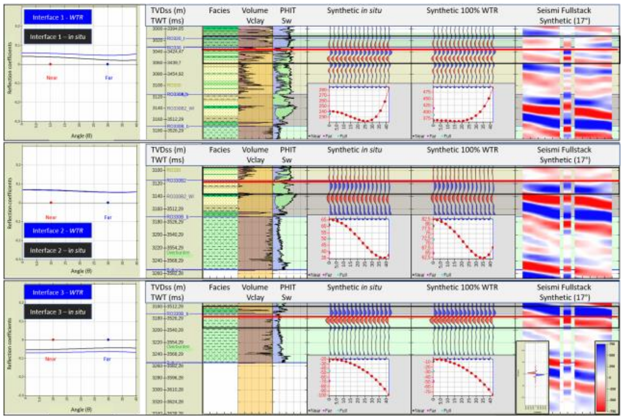

Figure 4 - Analysis of seismic amplitude based on the reflection coefficients for the interested interfaces.

In the interface 3, the synthetic amplitudes do not fit for mid and far angles. This is due to the wavelet characteristics because the seismic base lays down exactly 4ms delay. Figure 4 shows the modeled response for the seismic interface (inflection point). If the modeled seismic base reservoir (negative peak) including the time delay were considered, the reflection coefficients and synthetic amplitudes would fit as expected.

The class I response from interfaces 1 and 2, is responsible to dim the hard response due to hydrocarbon effects in seismic data. At interface 3, AVO responds to a class IV due to the hard sands found in this region.

The reflection coefficients modeling indicated that the Top and Base reservoir have a small difference to the values of modeled coefficients from both fluid scenarios. The coefficients for interface 2 present no variation between the modeled scenarios, indicating low sensitivity to fluids. This analysis can be an indicator of fluid sensitivity at the interfaces, in which it may provide important answers about the behavior of the elastic properties.

The elastic response from fluid scenarios was investigated in terms of the impedance contrasts (Figure 5). Thus, we verified which elastic attributes are more sensitive to fluids for the characterization of the reservoir RO330.

Figure 5 - Impedance contrast analysis between fluid scenarios per interfaces, showing the percentage variation of the scenarios.

The analysis of impedance contrasts, shows that some attributes are sensitive to fluids. This is noticeable for interfaces 1 and 3, where the analysis shown that the following attributes AI (Acosutic Impedance), EI2_30º (Elastic Impedance – 2Terms), K (Bulk Modullus), σ (Poisson's Ratio), λ (Shear Modullus), λρ (LambdaRho), λ/μ (LambdaOverRho) are the most sensible for fluid variation. The interface 2 does not show significant percentage variation between the scenarios. However, the impedance contrasts are significantly high when comparing with the interfaces 1 and 3. Thus, although these attributes are not sensitive to fluids in this interface, they can be useful in interpretation.

Analysis of elastic parameters based on lithofacies classification

In this step, the lithofacies were analyzed in terms of petrophysical properties (PHIT and Vclay) to understand their elastic responses. The relationship of lithofacies with the elastic attributes and petrophysical properties can be used to distinguish reservoir and non-reservoir facies. Figure 6 shows that some attributes can separate the lithofacies, although several impedances were sensitive to fluid variations at the interfaces.

Analyzing the histograms of the elastic attributes, we propose that AI and EI2_30º are the best attributes to separate the reservoir facies.

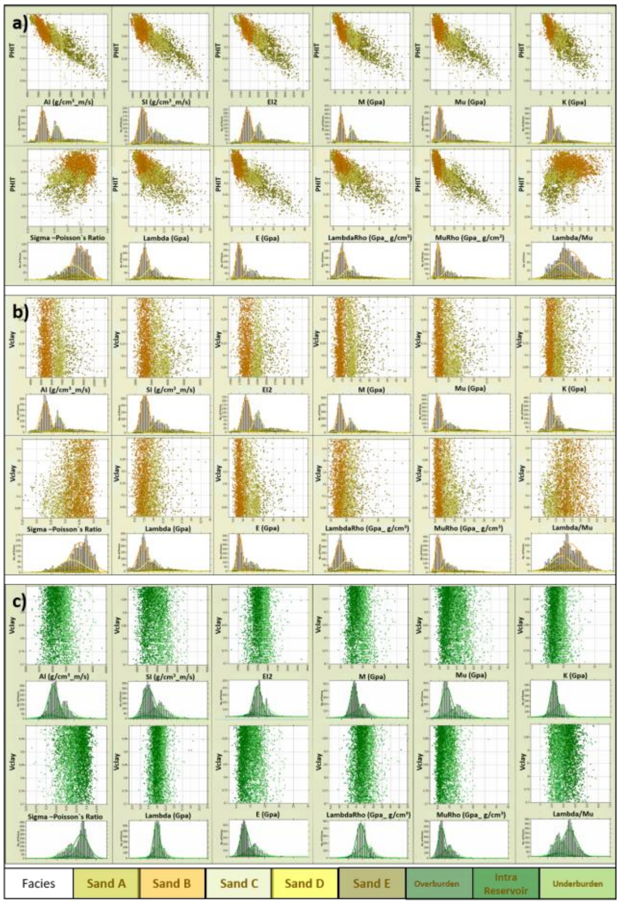

Figure 6 - Elastic attribute analysis parametrized by lithofacies for petrophysical properties. Reservoir facies are display in terms of PHIT (a) and Vclay (b). Non reservoir facies are display only for Vclay (c).

However, the elastic space of these two attributes shown that is not possible to distinguish the facies Sand D and Sand C. The other reservoir facies do not present significant overlap. For non-reservoir facies, none analyzed attributes providing a separation.

The AVO impedance technique (AVOI - Simm et al., 2002) proved be useful for the study area. This technique creates a projection of the Near and Far impedances (AI and EI2, in this case) by rotating the projection axis, generating a new elastic attribute. Figure 7 displays this process through a Weighted Stack Crossplot for reservoir rocks, with the projection as a function of Vclay. The relation that defines the separation of the reservoir rocks is given by:

$$\mathrm{Pjtn}_{\mathrm{rsv}} = -1.8823{*}\mathrm{AI} - \mathrm{EI2}(30°) + 13794{,}3. \qquad (1)$$

We extend this analysis to non-reservoir facies. Doing that, it was necessary, considering the reservoir facies, to obtain a relationship capable of separating them, once a relationship only for non-reservoir facies has proven to be quite ambiguous (Figure 8). However, we could obtain a relation for the Overburden and another one for the Underburden, given respectively, by:

$$\mathrm{Pjtn}_{\mathrm{Over}} = 0{,}2526{*}\mathrm{AI} - \mathrm{EI2}(30°) + 665{,}46 \qquad (2)$$

$$\mathrm{Pjtn}_{\mathrm{Under}} = 0{,}2455*\mathrm{AI} - \mathrm{EI2}(30°) + 693{,}47 \qquad (3)$$

From this analysis, we verify that Intra-reservoir and Sand D facies are indistinguishable from the Sand C facies. Also, shales from Overburden and Underburden intervals are totally overlapping. However, they assume values with a small range of variation, which in principle would allow a separation of the two facies (Figure 9).

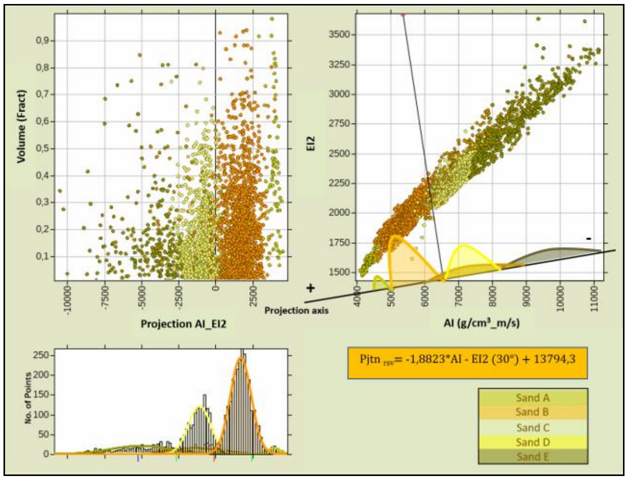

Figure 7 - Weighted Stack Crossplot displaying the analysis for all reservoir facies.

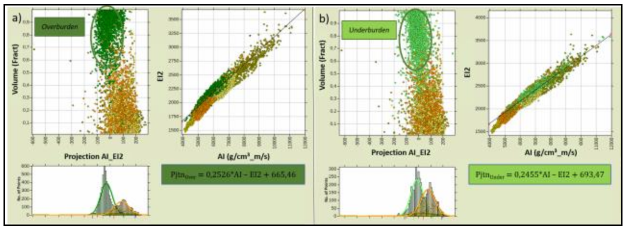

Figure 8 - Weighted Stack Crossplot displaying the analysis for non-reservoir facies Overburden (a) and Underburden (b).

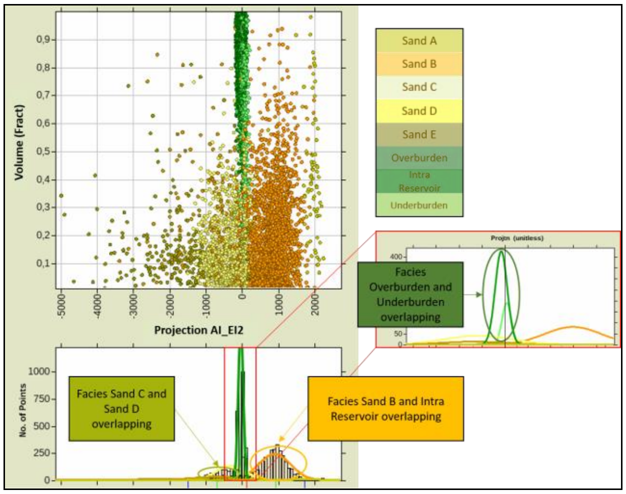

Figure 9 - Projection attribute analyzed by histograms for lithofacies.

Results

Our studies resulted in an elastic attribute calculated from AI_EI2 (30°) projection. Through the mathematical relationships described in Eqs. 1 to 3 defined for reservoir and non - reservoir facies, we generate an elastic attribute covering all the interested zones. Figure 10 displays the Discrimination Lithofacies Attribute (DLA) plotted alongside with the facies logs for some wells.

The DLA presented a good separation, considering the limitations discussed. Each lithofacies is associated to a specific range of attribute values, described according to Figure 11.

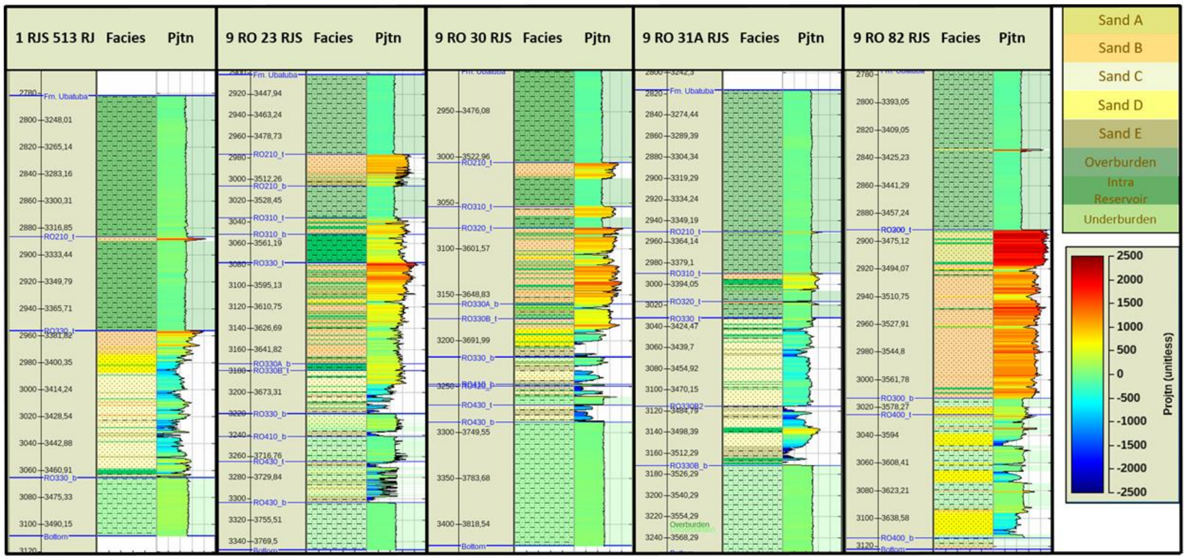

Figure 10 – Discrimination lithofacies attribute calculated over Wells 1 RJS 513 RJ, 9 RO 23 RJS, 9 RO 30 RJS, 9 RO 31A RJS and 9 RO 82 RJS are displayed together with lithofacies for comparison.

The DLA presented a good separation, considering the limitations discussed. Each lithofacies is associated to a specific range of attribute values, described according to Figure 11. Although Overburden and Underburden facies are overlapping with Sand C facies, it is possible to separate them, since non - reservoir Facies are separated by RO 330. For this situation, the discrimination was done through an interpretation of these intervals. Despite the overlapping, Overburden and Underburden Facies assumed different values due to analysis performed previously.

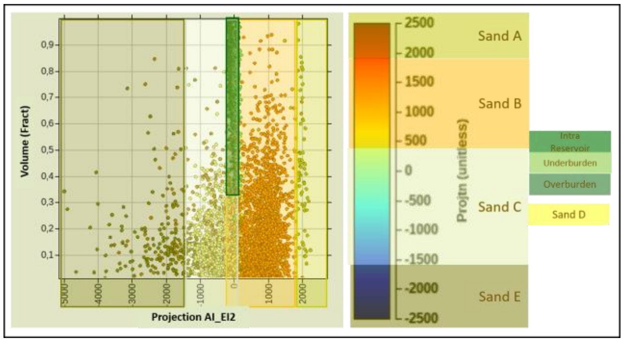

Figure 11 – Correlation among lithofacies distribution points and attribute values.

Conclusions

DLA obtained through the AVO Impedance (AVOI) technique captured the elastic and geological properties in the study area. From an elastic attribute, we perform a lithofacies classification according to the petrophysical properties (Vclay and PHIT). DLA proved to differentiate better the reservoir and non-reservoir facies when compared to the impedance attributes.

However, to minimize overlapping effects among lithofacies, a geological interpretation of the intervals is mandatory for the correct applications of this methodology and, consequently, for an adequate lithofacies characterization.

Once understanding the methodology limitations, in a strict low resources sense (time and people), this workflow can be applied in a fast and easy way as an alternative for the laborious and time consuming lithofacies characterization workflows from seismic impedances.

Acknowledgments

We thank Ikon Science Limited for providing access to the RokDoc software and the Agência Nacional do Petróleo, Gás Natural e Biocombustíveis (ANP) for providing data to perform this work.

References

AKI, K., RICHARDS, P. G., 1980. Quantitative Seismology.

ANP, 2020. Boletim da Produção de Petróleo e Gás Natural. Superintendência de Desenvolvimento e Produção - SDP. Agência Nacional de Petróleo. Março de 2020, n. 127.

AVSETH, P., MUKERJI, T., MAVKO, G., 2005. Quantitative Seismic Interpretation: Applying Rock Physics Tools to Reduce Interpretation Risk. Cambridge University Press, 359p.

BRUHN, C. H. L., GOMES, J. A. T., LUCCHESE JR, C. D., JOHANN, P. R. S., 2003. Campos Basin: Reservoir Characterization and Management – Historical Overview and Future Challenges. Offshore Technology Conference, OTC-15220-MS, Houston, Texas, USA, 5-8.

GASSMANN, F., 1951. On elasticity of porous media: Classics of elastic wave theory.

PÁDUA, K. G. O., STANK, C. V., SOARES, C. M., MOREIRA, J. V., 1998. Roncador Field, Strategy of Exploitation”. Offshore Technology Conference, OTC-8875-MS, Houston, Texas, USA, 4-7.

PAIVA, M. F. B., 2021. Modelagem de Física de Rochas e Análise dos Coeficientes de Reflexão e dos Atributos Elásticos dos Reservatórios Turbidíticos Maastrichtiano do Campo de Roncador, Bacia De Campos. Dissertação de mestrado. Programa de Pós Graduação em Dinâmica dos Oceanos e da Terra. UFF, Niterói.

RANGEL, H. D., MARTINS, C. C., 1998. Principais compartimentos exploratórios, Bacia de Campos. In: (ed) Searching for Oil and Gás in the Land of Giants. Rio de Janeiro, Schlumberger 32 – 40p.

SIMM, R., KEMPER, M., DEO, J., 2002. AVO Impedance: A new attribute for Fluid and Lithology Discrimination, Petex Conference, London.

WHITE, R. E., SIMM, R. W., 2003. Tutorial – good practice in well ties. First Break, 21, 75 – 83, 2003.